

A New Silver-Based Precursor as Ink for Soft Printing Techniques

Julia Fritsch,^[a] Benjamin Schumm,^[a] Ralf Biedermann,^[a] Julia Grothe,^{*[a]} and Stefan Kaskel^[a]

Keywords: Silver / Pyrrolidone / Photoreduction / Thin films / Patterning

A new, easily obtainable silver–pyrrolidone complex that is suitable for printing applications was synthesized by the reaction of silver nitrate and 2-pyrrolidone (Pyl) at room temperature. According to single-crystal X-ray crystallographic studies, the product $[\text{Ag}(\text{Pyl})_2]\text{NO}_3$ crystallizes in the monoclinic space group $C2/c$ (no. 15) [$a = 5.358(1) \text{ \AA}$, $b = 15.217(3) \text{ \AA}$, $c = 14.986(3) \text{ \AA}$, $\beta = 99.296(6)^\circ$]. Highly concentrated solutions of the complex can be obtained in an ethanol/water mixture, thereby allowing for the manufacture of

thin films by means of dip coating. Subsequent UV irradiation and moderate-temperature treatment yielded compact films of elemental silver with thicknesses of about 100 nm and sheet resistances down to 6.5Ω . Furthermore, microcontact printing (μcp) and embossing of $[\text{Ag}(\text{Pyl})_2]\text{NO}_3$ were performed, also followed by UV treatment. By means of the photoreduction of the complex and subsequent moderate-thermal treatment, defined structures of elemental silver lines were obtained.

Introduction

Transparent conductive films play a key role in several optoelectronic applications such as flat-panel displays, organic light-emitting diodes (OLEDs), and photovoltaics (PV).^[1–4] With increasing demand for structured transparent electrodes, printings of functional materials like transparent conductive oxides,^[5,6] conductive polymers,^[7] carbon-based materials,^[8,9] or metals^[10,11] have attracted much attention in recent years.^[12,13]

In particular, silver-based materials have been studied due to their advantages like very low resistivity, stability, and flexibility compared to transparent conductive oxides or polymers and carbon-based materials. However, the challenge in using silver is the fabrication of transparent materials. Due to that fact, several methods for the preparation of ultrathin films such as chemical vapor deposition or vacuum-thermal evaporation techniques have been investigated.^[14–16] Also, different printing techniques of metallic materials to obtain structured patterns with higher transparency have been reported recently. One way is to use simple metal solutions such as silver nitrate, which can be converted into silver at high temperatures (above 400°C).^[17] A second way is to use metallo-organic precursors or stabilized metal solutions, which can be converted into metals at lower temperatures.^[18–20] Another well-known method is the generation of silver-nanoparticle suspensions stabilized

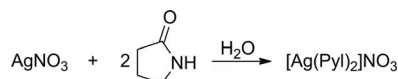
with polymers such as poly(*N*-vinyl-2-pyrrolidone) (PVP) or others.^[21,22] In addition to their stabilizing effect, PVP or pyrrolidone derivatives support the photoreduction of silver ions to elemental silver.^[23] Based on these conditions, we created an easily obtainable complex of silver nitrate and 2-pyrrolidone. Both silver nitrate and 2-pyrrolidone are highly soluble in water or water/ethanol mixtures. Similar to PVP, the organic 2-pyrrolidone ligand should have a stabilizing effect and support photoreduction. Due to these facts, the generated complex can be used as an ink for direct soft printing methods such as microcontact printing (μcp) or embossing processes that offer a way to fabricate conductive transparent substrates.

In the following we describe the structure of the new, easily obtainable silver complex synthesized by mixing silver nitrate and 2-pyrrolidone (Pyl) in water. In addition, we demonstrate its suitability as an ink by using dip coating for compact silver films and soft print methods for structured coatings.

Results and Discussion

Synthesis and Structural Characterization of $[\text{Ag}(\text{Pyl})_2]\text{NO}_3$

The reaction between aqueous solutions of silver nitrate and 2-pyrrolidone at room temperature under exclusion of light led to the formation of colorless crystals of $[\text{Ag}(\text{Pyl})_2]\text{NO}_3$ (Scheme 1).



Scheme 1. Synthesis of the $[\text{Ag}(\text{Pyl})_2]\text{NO}_3$.

[a] Department of Inorganic Chemistry, Dresden University of Technology
Bergstrasse 66, 01069 Dresden, Germany
Fax: +49-351-46337287
E-mail: Julia.Grothe@chemie.tu-dresden.de
Supporting information for this article is available on the WWW under <http://dx.doi.org/10.1002/ejic.201100930>.

The linear 1D polymeric silver complex poly-[Ag(PyI)₂]-NO₃ crystallizes in the monoclinic space group *C2/c* (no. 15) with four formula units per unit cell. The formula unit contains the 2-pyrrolidone molecules, one silver atom, and one nitrate anion. The silver atom and the nitrate anion occupy special positions on twofold axes. The Ag atom exhibits an irregular AgO₆ coordination geometry, which consists of two oxygen atoms from monodentate-coordinated 2-pyrrolidone molecules and four oxygen atoms from two bidentate-coordinated nitrate anions. The Ag–O distances are in the range of 2.358(2)–2.683(4) Å. The nitrate anions have a linker function and connect the structure into 1D polymeric chains, which are located along the [100] direction (Figure 1). The silver atoms are connected to a linear polymeric chain by μ₂-O bridging oxygen atoms O4 with a significantly longer Ag1–O4 distance [2.683(1) Å] than Ag1–O2 [2.536(4) Å]. In the crystal structure, the 1D polymeric chains are connected into the 2D network by intermolecular N–H···O hydrogen bonds (Figure 2) [N2–H3N···O1¹: D···A 2.952(4) Å, D–H···A 163°; *i*: 0.5 – *x*, 0.5 – *y*, –*z*].

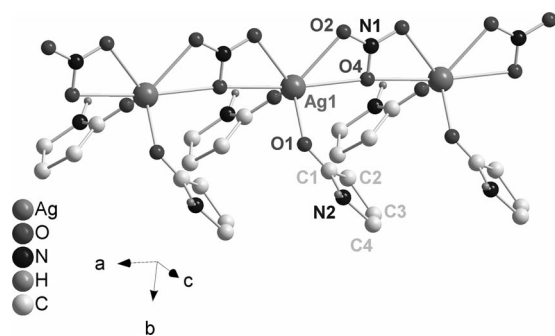


Figure 1. Linker function of the nitrate ion connecting the structure into 1D polymeric chains.

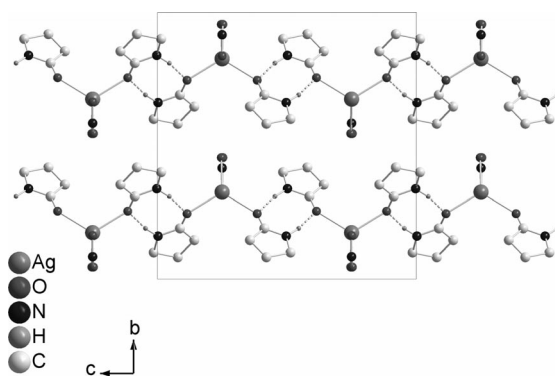


Figure 2. Two-dimensional network of [Ag(PyI)₂]-NO₃, which is connected through intermolecular N–H···O hydrogen bonds in the 1D polymeric chains.

As shown in Figure 3, the powder X-ray pattern of the silver complex conforms to the calculated one from the solved structure. The differences in intensity between several peaks are due to the preferred orientation of the acicular crystallites in the powdered sample. According to thermogravimetric analysis (see the Supporting Information),

the silver complex decomposes in two steps (see the Supporting Information, Figure a), whereas the major organic part (>60%) evaporates up to a temperature of 220 °C. This mass loss can be attributed to the 2-pyrrolidone ligand and parts of the nitrate. The second step at about 400–440 °C results in the volatilization of the residual nitrate. The final residue could be identified as elemental silver by using powder X-ray diffraction (PXRD) and supports the results from the elemental analysis (see the Supporting Information, Figures b and d).

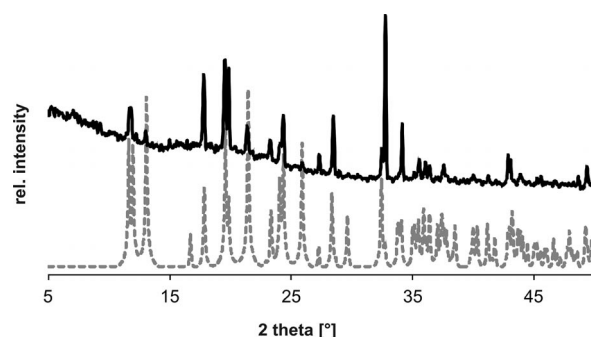
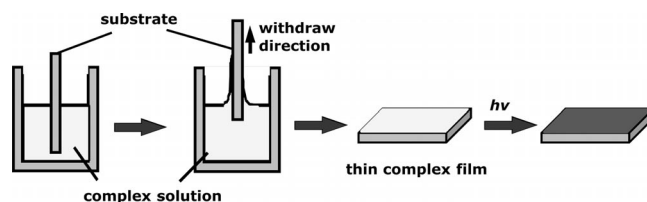


Figure 3. PXRD pattern of the silver complex (black) compared to the pattern that was calculated from the solved structure (dashed line).

Preparation of Compact, Thin Silver Films

The suitability of [Ag(PyI)₂]-NO₃ as an ink for the fabrication of thin, conductive silver films through soft printing techniques was tested by the preparation of thin, compact silver films. For this purpose, glass substrates were coated with an aqueous/ethanolic solution of the silver complex by means of dip coating (Scheme 2). Subsequently, the substrates were irradiated with UV light to obtain compact silver films. To achieve an optimal adhesion of the complex solution, the microscope slides were pretreated with a piranha solution. With this pretreatment, it was possible to obtain thin, homogeneously coated substrates.



Scheme 2. Schematic description of the dip-coating process to fabricate thin, compact silver coatings.

The photoreduction of the silver complex was examined by recording XRD patterns and SEM pictures after different periods of UV irradiation. As shown in the XRD of

Figure 4 (light gray line) and the respective photo, there is no complete conversion into elemental silver without UV irradiation. Additionally, the films are not homogeneous (Figure 5a). After 10 min of UV irradiation, elemental silver resulted (Figure 4, gray line), but as shown in the SEM image (Figure 5b), the layer is not homogeneous. An optimal silver coating was obtained after 20 min of irradiation (black line in the XRD of Figure 4, SEM image in Figure 5c). The broad signal in the thin-film XRDs from $2\theta \approx 20$ to 30° results from the glass substrate. Additionally, a thermogravimetric analysis of the UV-reduced sample was carried out (see the Supporting Information, Figure c). In contrast to the complex that was not irradiated, the decomposition took place in only one step at 220°C , and no further decomposition was observed at about $400\text{--}440^\circ\text{C}$, thus indicating the decomposition of the nitrate during the UV reduction. The residual mass fits the content of silver in a “nitrate-free” complex. Since the thermogravimetric analysis of the UV-reduced sample shows complete decomposition at 220°C , the coated substrates were additionally treated at a temperature of 220°C after UV irradiation. The necessity of this additional temperature treatment is demonstrated, for example, in a thicker layer with an UV-irradiation period of 20 min. As shown in Figure 6, the untreated layer (gray line) shows a slight crystallinity compared to the

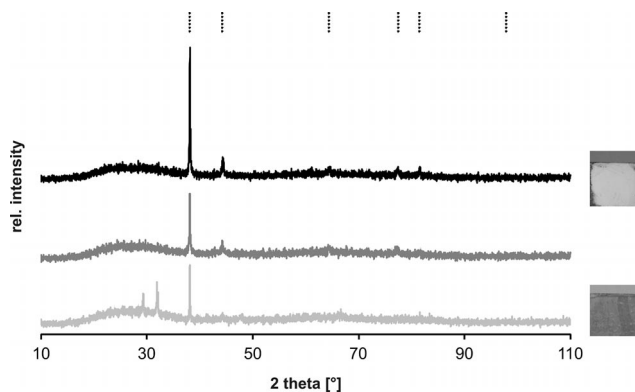


Figure 4. XRD patterns of the reduced complex with the following irradiation times: 0 min (light gray), 10 min (gray), 20 min (black); dashed lines: reference of silver [4-783]; photos of the substrates without UV irradiation (bottom) and after 20 min irradiation (top). Additionally, all coated substrates were treated at 220°C for 60 min.

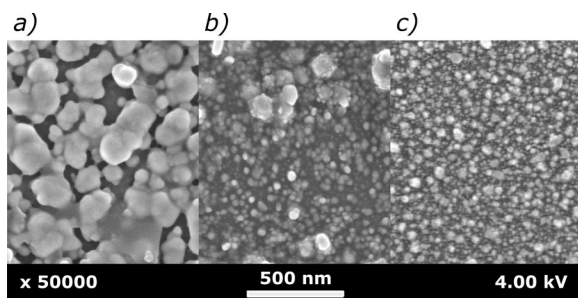


Figure 5. SEM images of the reduced complex with the following irradiation times: (a) 0, (b) 10, and (c) 20 min. All samples were treated after reduction at 220°C .

sample treated at 220°C (black line). Furthermore, without the temperature treatment, the dip-coated layers did not show good values in sheet resistance due to the presence of the organic ligand. To avoid an abrupt vaporization of any volatile components after UV irradiation, the samples were heated slowly to 220°C at a rate of 5 K min^{-1} .

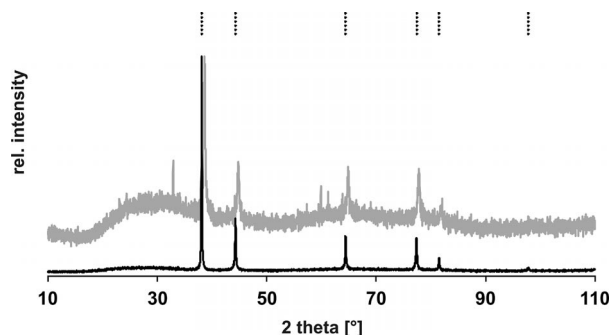


Figure 6. XRD pattern of the reduced complex without thermal treatment (gray) compared to that with thermal treatment (black); dashed lines: reference of silver ICSD [4-783].

To examine the thickness and surface morphology of the compact silver films, atomic force microscopy (AFM) and SEM measurements were used. In Figure 7a, an AFM image of a produced silver coating with optimized reduction conditions is shown. As seen in the picture, the surface of the film shows roughness. Surface roughness values were calculated with $R_a = 12.6\text{ nm}$ / $R_{ms} = 17.3\text{ nm}$. Due to that, the values of sheet resistance were measured by means of a four-point method spread between 6.5 and $20\ \Omega$ in one sample. However, for the calculation of the specific electrical resistance, we determined the thickness of the silver layers by means of AFM. In Figure 7b and c, the measurement of a scratch made with a scalpel with a resulting film thick-

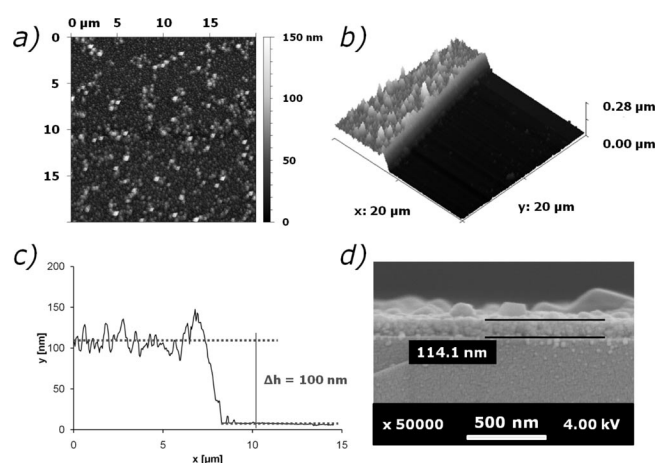
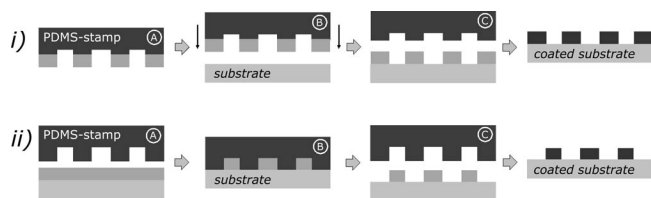


Figure 7. (a) AFM image of a compact dip-coated silver film that was UV-irradiated for 20 min and treated at 220°C ; (b) and (c) height profile of an AFM micrograph of the compact film scratched with a scalpel. The AFM cross section (c) shows the scratched zero level on the substrate and the silver film. To calculate the height, average values of both levels were estimated (dashed lines). (d) An SEM image of the edge of the silver film on the glass substrate with a determined film thickness of 114.1 nm .

ness of about 100 nm is shown. For the evaluation of the thickness, the values for both areas (the silver layer and the scratched area) were averaged (dashed lines) and the difference in height was estimated. By considering an average film thickness of about 100 nm, specific electrical resistances of $6.5 \times 10^{-7} \Omega\text{m}$ ($6.5 \times 10^{-5} \Omega\text{cm}$) to $2 \times 10^{-6} \Omega\text{m}$ ($2 \times 10^{-4} \Omega\text{cm}$, relative to the sheet resistances between 6.5 and 20 Ω) could be estimated. Compared to the resistance of the bulk material ($1.587 \times 10^{-8} \Omega\text{m}$),^[24] the films show a reduced performance that could be due to the roughness of the film surface but also grain boundaries in the nanoparticulate film with a mean particle size of about 40 nm [calculated from the single peak widths in the powder pattern of Figure 4 (black) and the SEM picture of Figure 5c]. To verify these results, SEM images at a cut edge of the silver film were recorded. As shown in the picture of Figure 7d, a film thickness of about 114 nm was examined, which is similar to the results of the AFM measurements. Slight differences are due to the surface roughness or the error limit of both methods.

Printed Silver Films

With the new silver complex, an ink for printing applications was synthesized. To prove this suitability, we tested the ink in soft printing techniques. We obtained patterned silver films with two different processes. In Scheme 3i, the microcontact printing (μcp) process is shown. The precursor solution was adjusted (A) with a polydimethylsiloxane (PDMS) stamp. Afterwards, the inked stamp was pressed onto the substrate (B) and the ink had to be transferred to the substrate (C). With a subsequent precursor–metal transformation, the silver-coated substrate could be obtained. By using a procedure similar to an embossing process (Scheme 3ii),^[13] the substrate could be coated with a compact precursor solution (A). Subsequently, the PDMS stamp was pressed into the compact film (B), and after removing a structured coating, the silver complex was obtained (C). Finally, a precursor–metal transformation resulted in the structured silver film.



Scheme 3. Schematical description of (i) the microcontact printing and (ii) the embossing process.

With both these soft printing processes, we were able to obtain structured silver coatings. To avoid crystallization of the complex during the printing process, a small amount (10 wt.-%) of an alkyl derivative of the ligand, 1-*tert*-butylpyrrolidin-2-one, was added to the reaction mixture. Figure 8a shows an optical microscope picture of silver lines with a line width of 20 μm and a distance of 20 μm between

the lines, which was printed by using the embossing technique. SEM measurements (Figure 8b) provide evidence of the compactness of elemental silver in the line that is comparable to the compact silver films (Figure 5c). The structuring can also be followed in an energy-dispersive X-ray (EDX) mapping (Figure 8c). For comparison, the mapping was made for silver and oxygen. As seen in the picture, silver is present only at the lines, and oxygen (from the glass substrate) is only visible between the lines. There are only minor amounts of silver between the lines due to an incomplete take-up of the ink in the printing process.

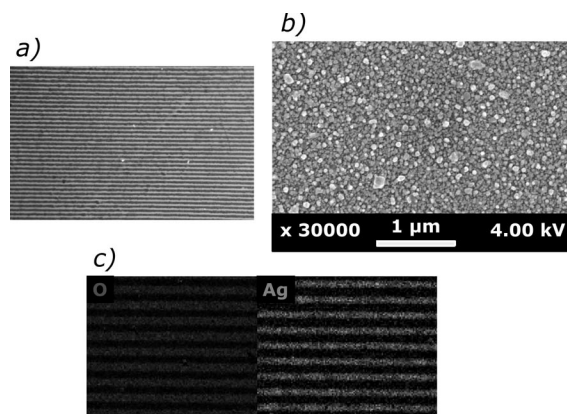


Figure 8. (a) Photo of the silver lines made by using an optical microscope. (b) SEM image measured in the line to show the compactness of silver in the lines. (c) EDX mapping of silver and oxygen on the structured substrate to show silver only in the printed area.

By using the μcp technique, it was also possible to obtain structured silver lines (Figure 9). On the left, an optical microscope picture of the obtained silver lines is shown. As seen in the picture, the line width is slightly enlarged relative to the distances between the lines, which could be due to smearing of the ink. That was previously observed in the embossing process but to a lesser extent. The structuring of silver was again verified by means of EDX mapping.

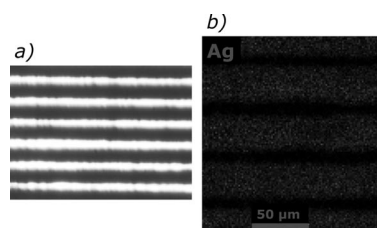


Figure 9. (a) Photo of the silver lines made by using an optical microscope. (b) EDX mapping on the structured substrate to show silver only in the printed area.

To conclude, patterned silver films could be obtained with both methods. With the embossing process, we were able to obtain homogeneous structuring. The compactness in the silver lines was included by using SEM analysis. EDX mapping shows silver only in the printed area. Minor amounts of silver between the lines could be due to an incomplete displacement or take-up of the ink. When using

the μcp technique, there is no silver between the lines but, as shown in Figure 9, the smearing of the ink is enlarged relative to the embossing process. With regards to the fabrication of transparent electrodes, the printing process has to be optimized in terms of the nano dimension of the line width.

Conclusion

A simple reaction was used for the synthesis of a silver-pyrrolidone complex. The preparation of colorless crystals of $[\text{Ag}(\text{Pyl})_2]\text{NO}_3$ was possible, and the corresponding crystal structure was solved and refined. Photoreduction by using UV irradiation and a subsequent thermal treatment at moderate temperatures allowed for the formation of elemental silver. This precursor-metal transformation was used in the preparation of thin compact films as well as structured silver films. For the compact silver coatings, we measured sheet resistances down to 6.5Ω on films irradiated with UV light for 20 min and treated at 220°C for 60 min. These values correspond to specific electrical resistances of down to $6.5 \times 10^{-5} \Omega\text{cm}$ by a calculated film thickness of about 100 nm. Structured silver coatings were obtained by using soft printing techniques.

Experimental Section

General Remarks: Triethylamine for the synthesis of *tert*-butylpyrrolidone was dried with CaH_2 . THF was dried with an M. Braun MB SPS-800 instrument. All other reagents and solvents were used as received without further purification. PXRD data were collected in transmission geometry with a Stoe Stadi-P powder diffractometer and $\text{Cu-K}_{\alpha 1}$ radiation. XRD patterns of thin films were recorded in Bragg-Brentano geometry with a Panalytical X'Pert Pro diffractometer, also with $\text{Cu-K}_{\alpha 1}$ radiation [$\lambda = 0.154(05) \text{ nm}$]. For crystallite size determinations, the single-line size/strain analysis (WinXPow, Stoe) was used. For correction of the instrumental broadening, a LaB_6 standard sample was used. The sheet resistance of compact silver coatings was measured by means of a four-point method with a Keithley 2400 source meter coupled with a four-point probe cascade by Cascade Microtech. For scanning electron microscopy (SEM) and energy-dispersive X-ray spectroscopy, a ZEISS DSM-982 Gemini was used. EDX evaluations of the films were performed by applying an acceleration voltage of 12 kV at a magnification of $1000\times$. The surface morphology and thickness of the silver films were evaluated with a Dimension 3100 atomic force microscope controlled by a Nanoscope IV SPM controller from Veeco Digital Instruments. The measurements were performed in tapping mode with a Veeco Nanoprobe RTESP7 tip. NMR spectra were recorded with a Bruker DRX 500 P (^1H : 500 MHz). Elemental analysis for the elements C, H, and N was performed with a CHNS 932 analyzer from Leco. The respective metal content was determined with an ICP-OES Vista RL apparatus from Varian Inc.

X-ray Crystallography: Single-crystal X-ray diffraction data for $[\text{Ag}(\text{Pyl})_2]\text{NO}_3$ were recorded with a Bruker APEX-II CCD and $\text{Mo-K}_{\alpha 1}$ radiation. The structure was solved and refined with the help of SHELX-97 software.^[25] Further details of the structural analysis are summarized in Table 1. CCDC-842454 ($[\text{Ag}(\text{Pyl})_2]$ -

NO_3) contains the supplementary crystallographic data for this paper. These data can be obtained free of charge from The Cambridge Crystallographic Data Centre via www.ccdc.cam.ac.uk/data_request/cif.

Table 1. Crystallographic data for $[\text{Ag}(\text{Pyl})_2]\text{NO}_3$.

	$[\text{Ag}(\text{Pyl})_2]\text{NO}_3$
Empirical formula	$\text{Ag}_1\text{C}_8\text{H}_{14}\text{N}_3\text{O}_5$
M_r	340.09
Space group (no.)	$C2/c$ (15)
a [\AA]	5.3583(10)
b [\AA]	15.217(3)
c [\AA]	14.986(3)
α [$^\circ$]	90
β [$^\circ$]	99.296(6)
γ [$^\circ$]	90
V [\AA^3]	1205.9(4)
Z	4
Reflections collected/independent	5080/1364
θ_{max}	27.50
GoF on F^2	1.098
R_{int}	0.0207
R_1, wR_2	0.0299, 0.0854
Max., min. peaks [$\text{e} \text{\AA}^{-3}$]	0.727, -0.471

Preparation of $[\text{Ag}(\text{Pyl})_2]\text{NO}_3$: Silver nitrate (0.34 g, 2 mmol, 99.5%, Sigma Aldrich) was dissolved in water (1 mL). 2-Pyrrolidone (0.34 g, 4 mmol, 99.0%, Sigma Aldrich) was added to the solution, and the mixture was stored under exclusion of light. The product was crystallized by slowly evaporating the solvent after a few days at room temperature.

Reduction of $[\text{Ag}(\text{Pyl})_2]\text{NO}_3$ and Preparation of Thin Films: To reduce the silver complex, solutions of $[\text{Ag}(\text{Pyl})_2]\text{NO}_3$ in ethanol/water (4:1) were prepared. Photoreduction was carried out by UV irradiation for 20 min. Subsequent treatment at $T = 220^\circ\text{C}$ yielded highly crystalline elemental silver. Compact films of silver were prepared by means of dip coating complex solutions (0.8 M) on pretreated glass substrates and subsequent reduction.

Synthesis of 1-*tert*-Butylpyrrolidin-2-one:^[26] THF (20 mL), triethylamine (3.5 g, 34.5 mmol, Acros Organics), and *tert*-butylamine (2.52 g, 34.5 mmol, 99.5%, Sigma Aldrich) were mixed in an argon-flushed flask and cooled to 0°C . 4-Chlorobutyl chloride (4.85 g, 34.5 mmol, 99.0%, Sigma Aldrich) was added very slowly under vigorous stirring, and the mixture was stirred at 0°C for 2 h. Afterwards, deposited triethylamine hydrochloride was filtered off, washed two times with THF (10 mL), and the filtrate was concentrated under reduced pressure. The raw product was mixed with ethyl acetate (90 mL), transferred into a separating funnel, and washed with HCl (1 M, 10 mL) and two times with brine (10 mL). The organic layer was dried with MgSO_4 , and the solvent was removed under reduced pressure.

The obtained *tert*-butyl-4-chlorobutanamide (6 g, 33.8 mmol) dissolved in THF (10 mL) was added to a solution of potassium *tert*-butoxide (3.9 g, 35 mmol, 99.99% sublimated grade, Sigma Aldrich) in THF (25 mL) with vigorous stirring very slowly at 0°C (Ar). After 2 h of stirring in an ice bath, the mixture was transferred into a separating funnel, mixed with ethyl acetate (50 mL), and washed two times with brine (20 mL). The organic layer was dried with MgSO_4 , and the solvent was removed under reduced pressure. After distillation under reduced pressure (14 mbar) at 75°C , the product was obtained as a colorless liquid (yield: 60%). ^1H NMR spectroscopic analysis provided evidence of the purity of the product compared to the data in the literature.^[26]

Nanoimprint Lithography (NIL) and Microcontact Printing (μ cp): Printed structures were fabricated with a GeSiM μ -contact printer 3.0. As stamp material, a Sylgard 184 PDMS cross-linked by standard procedure (1 h at 80 °C) was used. The silicon masters were manufactured by standard e-beam lithography techniques. To prepare defined structures, the solutions of the silver complex were printed on pretreated glass substrates by using μ cp and NIL techniques. Afterwards, the printed substrates were reduced analogously to the compact films.

Pretreatment of the Glass Substrates: To obtain an optimal adhesion for homogeneous thin films on the glass substrates, it was necessary to pretreat them. First, the glass slides were cleaned by sonication in ethanol for 15 min. Then they were placed in a piranha solution (1 part 30% H₂O₂, 3 parts concd. H₂SO₄) for 30 min. Finally, the slides were washed with MilliQ water and carefully dried under a slight nitrogen flow.

Supporting Information (see footnote on the first page of this article): TG analysis of the silver complex and the UV reduced sample, the elemental analysis of the silver complex, and a PXRD pattern of silver after the TG analysis.

Acknowledgments

This work was fully funded by the European Social Fund (ESF) and the Free State of Saxony (project no. 080940507).

- [1] K. L. Chopra, S. Major, D. K. Pandya, *Thin Solid Films* **1983**, *102*, 1–46.
- [2] S. Calnan, A. N. Tiwari, *Thin Solid Films* **2010**, *518*, 1839–1849.
- [3] H. Liu, V. Avrutin, N. Izyumskaya, Ü. Özgür, H. Morkoç, *Superlattices Microstruct.* **2010**, *48*, 458–484.
- [4] C. G. Granqvist, *Sol. Energy Mater. Sol. Cells* **2007**, *91*, 1529–1598.
- [5] B. Schumm, P. Wollmann, J. Fritsch, J. Grothe, S. Kaskel, *J. Mater. Chem.* **2011**, *21*, 10697.
- [6] H. Stiebig, N. Senoussaoui, C. Zahren, C. Haase, J. Müller, *Prog. Photovolt. Res. Appl.* **2006**, *14*, 13–24.
- [7] C. Liu, C. Huang, S. Wu, J. Han, K. Hsieh, *Polym. Int.* **2010**, *59*, 517–522.
- [8] Q. Cao, J. A. Rogers, *Adv. Mater.* **2009**, *21*, 29–53.
- [9] M. Bansal, R. Srivastava, C. Lal, M. N. Kamalasanan, L. S. Tanwar, *Nanoscale* **2009**, *1*, 317.
- [10] M.-G. Kang, L. J. Guo, *Adv. Mater.* **2007**, *19*, 1391–1396.
- [11] J.-T. Wu, S. L.-C. Hsu, M.-H. Tsai, W.-S. Hwang, *Thin Solid Films* **2009**, *517*, 5913–5917.
- [12] Y. Xia, G. M. Whitesides, *Annu. Rev. Mater. Sci.* **1998**, *28*, 153–184.
- [13] E. Menard, M. A. Meitl, Y. Sun, J.-U. Park, D. J.-L. Shir, Y.-S. Nam, S. Jeon, J. A. Rogers, *Chem. Rev.* **2007**, *107*, 1117–1160.
- [14] T. Struppert, A. Jakob, A. Heft, B. Grünler, H. Lang, *Thin Solid Films* **2010**, *518*, 5741–5744.
- [15] R. B. Pode, C. J. Lee, D. G. Moon, J. I. Han, *Appl. Phys. Lett.* **2004**, *84*, 4614.
- [16] A. Jakob, T. Ruffer, H. Schmidt, P. Djiele, K. Körbitz, P. Ecorchard, T. Haase, K. Kohse-Höinghaus, S. Frühauf, T. Wächtler, S. Schulz, T. Gessner, H. Lang, *Eur. J. Inorg. Chem.* **2010**, 2975–2986.
- [17] Z. Liu, Y. Su, K. Varahramyan, *Thin Solid Films* **2005**, *478*, 275–279.
- [18] A. L. Dearden, P. J. Smith, D.-Y. Shin, N. Reis, B. Derby, P. O'Brien, *Macromol. Rapid Commun.* **2005**, *26*, 315–318.
- [19] J. J. P. Valetton, K. Hermans, C. W. M. Bastiaansen, D. J. Broer, J. Perelaer, U. S. Schubert, G. P. Crawford, P. J. Smith, *J. Mater. Chem.* **2010**, *20*, 543.
- [20] J.-T. Wu, S. L.-C. Hsu, M.-H. Tsai, W.-S. Hwang, *J. Phys. Chem. C* **2010**, *114*, 4659–4662.
- [21] S. L.-C. Hsu, R.-T. Wu, *Mater. Lett.* **2007**, *61*, 3719–3722.
- [22] M. Layani, M. Gruchko, O. Milo, I. Balberg, D. Azulay, S. Magdassi, *ACS Nano* **2009**, *3*, 3537–3542.
- [23] W.-F. Lee, K.-T. Tsao, *J. Mater. Sci.* **2009**, *45*, 89–97.
- [24] D. R. Lide, *CRC Handbook of Chemistry and Physics*, CRC Press, Taylor & Francis, Boca Raton, Florida, **2009**.
- [25] *SHELXS-97: Programs for Crystal Structure Solution*: G. M. Sheldrick, *Acta Crystallogr., Sect. A* **2008**, *64*, 112–122.
- [26] K. Takao, K. Noda, Y. Morita, K. Nishimura, Y. Ikeda, *Cryst. Growth Des.* **2008**, *8*, 2364–2376.

Received: September 2, 2011
 Published Online: January 3, 2012